Cardiotoxic effects of methamphetamine associated with electrophysiological and epigenetic aberrations in zebrafish

Jimmy Zhang[1†], Anh H. Nguyen[2,3*†], Lauren Schmiess-Heine[2], Tai Le[1], Xing Xia[2], Michael P.H. Lau[3], Juhyun Lee[4], Hung Cao[1,2,3*]

[1]Department of Biomedical Engineering, UC Irvine, Irvine, CA 92697, USA.

[2]Department of Electrical Engineering and Computer Science, UC Irvine, Irvine, CA 92697, USA.

[3]Sensoriis, Inc, Edmonds, WA 98026, USA.

[4]Department of Bioengineering, University of Texas, Arlington, TX, 76019, USA.

[†]*Equal contribution*

**Co-corresponding authors*

Correspondence

Hung Cao, Ph.D.

Assistant Professor of Electrical and Biomedical Engineering

University of California, Irvine

Irvine, CA 92697

E-mail: hungcao@uci.edu

Abstract

Long-term methamphetamine (Meth) abuse damages functional and molecular changes in the brain that causes chronic and relapsing disease. In this study, we sought to investigate a relationship between cardiotoxicity and arrhythmia with associated Meth abuse in zebrafish to identify and to understand the adverse cardiac symptoms associated with Meth as well as to assess the applicability of zebrafish as an appropriate model for cardiac-related drug screening studies. Over a two-week duration, zebrafish were first treated with various concentrations of Meth, ranging from 0 to 50 μM. Immediately after treatment, zebrafish underwent electrocardiogram (ECG) measurement for electrophysiological analysis. Results show that a higher incidence of increased heart rate over the duration of the experiment, corroborating with results from previous human case studies involving Meth users. However, abnormalities commonly cited in those same case studies, such as prolongation of QTc, were not significantly presented in obtained ECG recordings. We have also conducted genetic, epigenetic, and histochemical analysis in an attempt to understand the cardiotoxic effects of Meth on zebrafish cardiac function. These results suggested myocardial damage and decrease in gene expression associated with normal physiological function. Finally, this paper provides insights into potential reasons for the apparent discrepancies in our data with prior research as well as an outlook of zebrafish cardiotoxic drug screening studies.

41 # Introduction

42 Cardiotoxicity is one of the most adverse consequences of methamphetamine (Meth)
43 abuse, leading to a notable increase of morbidity and mortality (1). Cardiovascular complications
44 are the second leading cause of death in Meth abusers. Cardiotoxicity can appear early in the
45 course of drug use and can cause numerous significant effects, such as pulmonary
46 hypertension, atherosclerosis, cardiac arrhythmias, acute coronary syndrome, and other
47 associated cardiomyopathies (2). Furthermore, a Meth 'binge' study to determine long-term
48 effects discovered that Meth decreased the sensitivity of nervous and cardiovascular physiology
49 through successive treatments, implying the potential remodeling of physiological responses
50 through chronic Meth abuse (3). However, data on the mechanism of the appearance of cardiac
51 dysfunction during drug abuse and the susceptibility of long-term development of cardiotoxicity
52 are limited. Therefore, further investigation of Meth abuse and early diagnosis of pre-clinical
53 cardiac dysfunction in zebrafish, a relevant model for human cardiac studies, is essential in order
54 to understand Meth-induced cardiac toxicity.

55 Meth is a sympathomimetic amine with a range of adverse effects upon multiple organ
56 systems. Based around a phenylethylamine core, Meth and its analog, *d*-amphetamine, have
57 high affinity with transporters associated with catecholamine signaling, significantly increasing
58 the number of neurotransmitters such as dopamine and norepinephrine (1). Unlike Meth, *d*-
59 amphetamine has been prescribed as medication to treat neurological disorders such as
60 attention deficit hyperactivity disorder (ADHD) and narcolepsy (4). A possible reason for limited
61 legal Meth use is the addition of the *N*-methyl group compared to amphetamine, which has been
62 shown to confer better penetration through the blood-brain barrier for Meth, leading to stronger
63 and more addictive responses (5). Meth has been shown to induce heightened catecholamine
64 response by promoting catecholamine release, preventing their reuptake, and destabilizing their

levels (6, 7). Thus, Meth is responsible for numerous neurotoxic symptoms (7). Given the elucidation of the direct mechanism of Meth on neurological response, the major focus in researching treatments for Meth-related abuse has been associated with neurological modulation. Therefore, less attention was given to researching the direct mechanism of Meth in other physiological systems, such as the cardiovascular system.

Despite the prevailing issue of Meth abuse, studies have shown that cardiac pathology induced by Meth can be attenuated and even reversed through the discontinuation of Meth use and the initiation of subsequent treatment (8). A study in rats regarding the administration of Meth and eventual withdrawal revealed that the rats were able to recover from myocardial pathologic symptoms such as atrophy, fibrosis, and edema starting from 3 weeks after discontinued Meth administration (9). A human case study indicated that attenuation of Meth use and subsequent therapy led to recovery from ventricular hypertrophy and electrocardiogram (ECG) ST deviations (10). Evidence of recovery from Meth abuse has given promise to future potential treatments, but it also necessitates the research to understand the specific mechanism behind Meth-induced cardiovascular pathologies.

Zebrafish has recently emerged as an efficient low-cost animal research model that has been used for high-throughput phenotype-driven drug screenings for new insights into chemical toxicity due to similar drug metabolism and genetic homology (11). Although current research has not fully proven whether the single ventricular heart of zebrafish is comparable to the more complex ventricular conduction system found in higher vertebrates, zebrafish have been proposed as a versatile model system for biological studies due similarities with humans pertaining to cardiac physiology. Our group has reported the use of *in vivo* surface ECG in adult zebrafish for monitoring irregular heartbeats and QT prolongation (12). Here, we further demonstrated ECG screening in adult zebrafish as a powerful tool for cross-sectional and longitudinal studies for Meth-induced cardiac toxicity. Specifically, we established techniques

90 that allow for the accurate and reproducible detection of irregular arrhythmic symptoms, enabling
91 early ECG-based detection of cardiac dysfunction for drug abusers, further defining ECG as a
92 suitable benchmark test for the extent of Meth-induced cardiotoxicity.

93 Materials and methods

94 Zebrafish husbandry and experimental preparation

95 Wild-type zebrafish were housed in a custom-built circulating fish rack system. The water
96 environment was maintained at 28˚C, ~pH 7.0, and was checked at least once daily. The system
97 is equipped with four filters, a UV, carbon, and two particle filters. Zebrafish were kept under the
98 14:10 hour light/dark cycle. All zebrafish used in this study were wild-type strain obtained from
99 the UC Los Angeles aquatic facility and were approximately 1 year old at the onset of the
100 experiment. Prior to Meth treatment, zebrafish underwent open chest surgery to improve
101 subsequent ECG signal acquisition (12). Under a stereo microscope, scales (above the coelomic
102 cavity and the posterior site above the tail) were removed with forceps, exposing flesh, to allow
103 more direct electrode contact. A small incision, ~2-3 mm, was made on the ventral surface of
104 the fish above the heart. The incision cut through the chest wall and the heart was visible
105 afterward. The fish were recovered in fresh fish water for a few minutes. The incision was not
106 closed via suture, staple, clips, or glue as chest wall and scales have been observed to regrow
107 within 4 weeks. Fish will regrow scales and recover fully within 4 weeks. The 4 zebrafish groups
108 were then housed in separate tanks throughout the duration of the study. Fish were checked
109 every day until the experiment has concluded, to see whether the animal was slow or showed
110 some abnormal activities (*i.e.*, erratic swimming, strained breathing, bloating). In those cases,
111 the fish would be euthanized in accordance to UC-Irvine's Institutional Animal Care and Use
112 Committee (IACUC) guidelines (Protocol # AUP-21-066).

113

114 Drug preparation and Meth treatment

115 The various concentrations (0, 25, 40, and 50 μM) of Meth solutions for treatment were
116 prepared by mixing the specified amount of Meth stock into water obtained from the fish rack
117 system on the day of treatment. The Meth stock (1 mg/mL) was obtained from Sigma-Aldrich
118 (MDL MFCD00056130). The solution (~10 mL) was then placed in a small custom PDMS
119 chamber suitable for housing one zebrafish. Each zebrafish was treated in the designated
120 concentration of Meth solution for 20 minutes before ECG recording.

121 ECG recording procedure and instrumental setup

122 ECG was obtained using the instrumental setup depicted in **Fig 1a**. Prior to placing the
123 fish in the designated zebrafish station, the fish was first anesthetized in tricaine (200 mg/L) for
124 approximately 3 minutes until the fish became unresponsive to external stimulus. Then, the fish
125 was placed ventral side up in a precut crevice in the middle of the sponge. The sponge was then
126 placed on a glass platform with the pin electrodes as positioned in **Fig 1a**, where the green
127 working electrode was placed near the open incision on the chest while the yellow reference
128 electrode was placed near the lower abdomen. Each fish underwent recording for approximately
129 1 minute before placing in regular fish water for recovery from anesthesia. Treatment
130 concentrations and durations were approved by University of California-Irvine's IACUC.

131

Fig. 1. Zebrafish ECG Setup. (a) The figure on the left shows the general layout of zebrafish and electrodes during ECG recording. The working electrode is shown in green and contacts the chest cavity. The reference electrode is shown in yellow and contacts near the tail. This electrode setup connects with instruments outlined in the block diagram on the right, where signals are processed and displayed on the laptop. The islet provides a closer view of the positioning of electrodes on the zebrafish during recording. (b) Representations of ECG signal processing with labeled waveforms utilizing custom Matlab software. The top displays the orange raw signal, while the bottom displays the blue processed signal.

132 The components of instrumental setup consisted of the following (**Fig 1a**). The pin
133 electrodes were derived from isolating ends of jumper wires (Austor Part AMA-18-580) and
134 stripping the outer insulator layer of the wire about 2 cm from the metal tip of the wires. The
135 exposed copper wire underneath was then soldered to improve signal integrity and electrode
136 longevity. The pin electrodes were attached to alligator clips at the end of a cable wire leading
137 to the differential AC amplifier (A-M Systems Model 1700). The connecting cable was wrapped
138 with aluminum foil and grounded to reduce external electrical noise. The signal from the
139 zebrafish underwent 10000x amplification before undergoing digitalization with the data
140 acquisition box (National Instruments Model USB-6001). The signal was then transmitted to a
141 laptop (Dell Latitude E5470), where the processed ECG signal was displayed using the LabView
142 interface. Examples of ECG recordings are shown in **Fig 1b**.

143

144 ECG data collection and analysis

145 ECG signals were saved as a text file using the LabView interface. The ECG was
146 subsequently analyzed using a custom-designed MATLAB software to determine the positions
147 of ECG waves for each recording(13). Briefly, the MATLAB m-file first loaded and plotted the
148 ECG data from the output text file from LabView. The m-file then determined locations of peaks
149 corresponding to R waves via local maximum detection. After a denoising step, the P waves,

150 QRS complexes, and T waves were then determined based on predetermined parameters and
151 deviations from the R waves. Finally, relevant statistics such as the QTc duration based on the
152 Bazett formula and heart rate (HR) were calculated and tabulated in an output Excel file
153 corresponding to each ECG data file (14). Prior to subsequent analysis, each data file was
154 reviewed for accurate ECG wave detection by determining that the locations of P, Q, R, S, and
155 T waves depicted by the software conform to the corresponding peaks/troughs on the ECG.

156 Bazett formula: $QTc = \frac{QT\ Interval}{\sqrt{RR\ Interval}}$

157 RT-PCR analysis

158 Zebrafish were euthanized and homogenized. RNA was successfully isolated following
159 the TRIzol® reagent protocol (Invitrogen). Subsequent first strand synthesis of cDNA was
160 conducted following the protocol of M-MLV reverse transcriptase (Promega). qPCR was
161 conducted with SYBR-Green reagent and analyzed with the Quantstudio Real-Time PCR
162 System. DNA primers used for qPCR are shown in **Table 1**.

163 **Table 1. List of primers used for RT-PCR**

Name	Accession No. (NCBI)	Product size (bp)	Primer Sequence
MBD3	NM_212769.1	120	F: 5′-GTCCAACAGGGAAGAAG-3′ R: 5′-GGCAGAGACGTGTTCAG-3′
MBD2	NM_212768.1	105	F: 5′-GAGCTCAGCAGCTAGC-3′ R: 5′-CCGTCCTCTTCTTCTC-3′
MBD1	BC124166.1	102	F: 5′-GAAGGTGAAGATGC-3′ R: 5′-TTCAGCTTCTTCAC-3′

PRMT4	NM_001007183.2	98	F: 5′-GAAGCTGCACTGGT-3′ R: 5′-GTGGAACTCGTATC-3′
NNMT	NM_001372046.1	105	F: 5′-GACATCGGCTCTGGC-3′ R: 5′-CAGCACCTGCTTGAC-3′
LCMT1	NM_001004645.2	105	F: 5′-CACCTGAGATCAACAG-3′ R: 5′-GGTTTCGATAGTGGAG-3′
EHMT2	NM_001113615.1	120	F: 5′-GAGACAGAGCCGCAGC-3′ R: 5′-GAGACTGTCTGCTGCT-3′
EHMT1b	XM_021468789.1	109	F: 5′-GCCAAGGACCAAGTC-3′ R: 5′-CGTGCACGATGTACTG-3′
COMTA	NM_001030157.2	112	F: 5′-CACGATGTGGTCCATC-3′ R: 5′-GCGATGACGCTCTCTG-3′
DMNT3a	NM_001328167.1	103	F: 5′-CACTCCACGCTGGAC-3′ R: 5′-TCGTCGCACTTCTCC-3′
DMNT3b	NM_001020476.2	98	F: 5′-GAAGCTCGTGATGGTC-3′ R: 5′-TGTCAGACTCTTCTC-3′
DMNT1	NM_131189.2	110	F: 5′-GCCTGAAGCTGAGAATGC-3′ R: 5′-CTCATCGGTTAACATCTC-3′
KCNH2	NM_001044931.1	103	F: 5′-CACCTGGGACTGGGTGATC-3′ R: 5′-TGTGGAAATTCAGCACAAT-3′
KCNQ1	NM_001123242.2	112	F: 5′-GATGCCGGAGTAAATATGT-3′ R: 5′-GGACTCCTCTGACAGCAG-3′
SCN5A	NM_198056.3	110	F: 5′-GGAACTGGCTGGACTTTAG-3′

			R: 5′-CTGGATCAGGGCCCCCACG-3′

164

165 ## Protein extraction and dot blot analysis

166 After treatment of zebrafish with Meth concentrations of 25, 40, and 50 μM, the zebrafish
167 were euthanized and homogenized. Their proteins were extracted with the TRIzol® reagent and
168 protocol (Invitrogen). In brief, whole zebrafish (~400 mg) are gently pipetted in a 1.5 mL
169 Eppendorf (EP) tube. The zebrafish tissues were homogenized by liquid nitrogen before being
170 incubated in 1 mL TRIzol® on ice for 5 min. The extract was centrifuged at 13,000 rpm at 4°C for
171 45 min and the supernatant was collected into a fresh 1.5 mL EP tube. 200 μL of Chloroform
172 was added and mixed thoroughly, left the tube on ice for 5 min, and centrifuged at 13,000 rpm
173 at 4°C for 15 min. After removing aqueous phase for RNA and precipitating DNA by ethanol,
174 proteins were precipitated by adding 1.5 mL isopropanol, mix thoroughly and incubate for 10 min
175 at room temperature. The extract was centrifuged at 12,000 rpm at 4°C for 10 min, supernatant
176 was discarded. 2 mL of 0.3 M guanidine hydrochloride solution was added and incubate for 20
177 min at room temperature. The sample was centrifuged at 12,000 rpm at 4°C for 5 min, discard
178 the supernatant. The protein pellet was washed with 2 mL of ethanol and dried for 5 min. The
179 protein pellet was resolubilized with 1mL of 1% SDS solution, the supernatant was collected
180 after centrifuge at 12,000 rpm at 4°C for 10 min, ready to use for subsequent protein analysis.
181 Extracted proteins were dissolved in 1% SDS. The protein solution was then dropped on a
182 nitrocellulose membrane (GE Healthcare Protran® BA85) to form 2 μL and 5 μL dots for each
183 concentration group. After 1 hour of incubation, the membrane was then blocked with TBST
184 including 1% BSA for 1 hour, followed by an overnight incubation with the anti-Meth antibody
185 (mouse, 10M25A Fitzgerald). After washing the membrane with TBST, the membrane was then
186 incubated with HRP conjugated anti-mouse IgG (R&D Systems) for 4 hours. After additional

187 washing, the membrane was then incubated in Pierce™ ECL Western Blotting Substrate
188 (Thermo Scientific) and imaged for chemiluminescence.

189 Histochemical staining with Masson's trichrome stain

190 After treatment of Meth, zebrafish hearts were isolated as described in previous literature
191 (15). Briefly, the fish were anesthetized by tricaine before undergoing chest incisions. The heart
192 was then located and excised, which were then placed in a solution of perfusion buffer (10 mM
193 HEPES, 30 mM taurine, 5.5 mM glucose and 10 mM BDM in 1x PBS solution). After excision of
194 all hearts, they were subsequently fixed by 4% formaldehyde and cryo-sectioned with a cryostat.
195 The tissue slices were placed onto frosted microscope slides (Thermofisher Scientific) and
196 underwent Masson's Trichrome staining (following the provided protocol from American Master
197 Tech, TKMTR2). The slides were observed under the microscope for subsequent analysis of
198 collagen and myocardium distribution for cardiac injury analysis.
199

200 Antibodies for immunostaining and ELISA analysis

201 Protein extraction by TRIzol® reagent was conducted prior to ELISA. Heart tissue samples
202 were fixed and sectioned with the aforementioned procedure prior to immunostaining. The
203 antibodies used for immunostaining and ELISA were mouse anti-Meth antibody (mouse,
204 10M25A Fitzgerald), anti-MBD2 (ab45027; Abcam), anti-DNMT1 antibody (mouse, ab13537;
205 Abcam) and the secondary antibodies used were goat anti-mouse IgG-HRP (ab6789; Abcam),
206 goat anti-mouse IgG H&L (Alexa Fluor® 488) (ab150113, Abcam).

207 ## Statistical analysis

208 All parameters derived from data analysis (*i.e.,* QTc, HR) were averaged within each
209 experimental group. Statistical significance was determined by the one-way ANOVA test
210 between experimental groups with significance level $p<0.05$.

211 # Results

212 ## Significant dose-response increase in heart rate but not in QTc
213 ## from Meth treatment

214 Zebrafish has been a favorable model for drug screening experiments, including Meth.
215 Indeed, most studies regarding zebrafish Meth treatment concern the neuropsychological effects
216 of Meth, owing to the ability of Meth to enhance catecholamine neurotransmitters (16, 17).
217 Studies of zebrafish cardiotoxicity in response to Meth administration are scarcer. Fang *et al.*
218 conducted a Meth cardiotoxicity study by treating 48 hpf (hours post fertilization) zebrafish
219 embryos with up to 24 hours of Meth administration, documenting decreased heart rate and
220 abnormal morphological changes such as edema and hemorrhage (18). To this end, we sought
221 to verify and expand on their results through our methodology in ECG acquisition, as arrhythmia
222 was a prominent cardiotoxic symptom in Meth abusers (1). Our lab previously developed
223 modalities in acquiring ECG from adult zebrafish and successfully identified abnormal ECG
224 characteristics (12). Using an ECG setup designed in our lab (**Fig 1**), we acquired ECG signals
225 over a two-week period. Each experimental group is treated with the designated Meth
226 concentration for 20 minutes for 3 instances per week, and their ECG was subsequently acquired
227 after treatment. The signals were then processed to eliminate external noise, and parameters

228 such as heart rate and QTc were then quantified. **Fig 2a** comprises representative ECG figures
229 obtained from our ECG system, including ECG diagrams obtained before Meth administration
230 as well as 7 days and 14 days after first administration. **Fig 2b** is a representation of a pathogenic
231 progression of ECG signals due to Meth treatment. The evident increase of heart rate and
232 sporadic signs of QTc prolongation were seen after the first and second weeks of treatment.
233 Through our analysis of ECG recordings of zebrafish treated at varying concentrations of Meth
234 over the period of 2 weeks, a significant increase in heart rate was noted for all zebrafish groups
235 treated with Meth compared to zebrafish not treated with Meth (**Fig 2a**), which is consistent with
236 previous studies of Meth users displaying monomorphic ventricular tachycardia (19). However,
237 our data indicated that significant QTc prolongation did not occur due to Meth treatment (**Fig 3**).
238 This seemingly contradicts with results obtained from previous human medical case studies, as
239 those cases reported significant signs of QTc prolongation in Meth users (20, 21). Comparison
240 between heart rate and QTc for individual measurements (**Fig 3a**) revealed that there was no
241 significant correlation between heart rate and QTc. Furthermore, heart rate tended to display a
242 wider range of values than for QTc across treatment groups, supporting the previous analysis
243 that Meth induces a more significant change in heart rate than in QTc. Heart rate values for each
244 treatment group were more delineated, as values from the control group were colocalized at the
245 lower range of heart rates (mean = 87.4 bpm), whereas values from the 50 μM treatment group
246 were colocalized at the higher range (mean = 94.6 bpm). QTc results did not display the same
247 discrimination as in heart rate, as values were congregated regardless of experimental group.
248 This was corroborated by measuring the variation in heart rate in each group, as the variations
249 remain relatively similar regardless of experimental treatment. While some outliers populated
250 the high extreme values of QTc, the majority of QTc values were congregated.

251 ## Lack of significant differences in ECG characteristics between
252 treatment groups

253 While significant differences can be found for heart rate between zebrafish treated and not
254 treated with Meth, other characteristics, including ST intervals and RR intervals, do not show
255 significant correlation. According to the odds analysis shown in **Fig 3d**, only QTc, heart rate, and
256 RTc have shown significant differences between Meth-treated and untreated groups (OR > 2.5).
257 A closer inspection of the odds ratios indicate that the significance was fairly weak for RTc and
258 QTc, which was corroborated by T-tests conducted above. Other parameters that were studied,
259 such as ST interval, have an odds ratio below the significant value.

Fig 2. Analysis of ECG before and after treatment. (**a**) This representative figure indicates the ECG signals before treatment, labeled as 'Baseline', as well as signals obtained at 7 and 14 days after the onset of methamphetamine treatment. ECG waveforms were labeled for the initial ECG wave. The progression of ECG signals depicts an increase in heart rate after onset of treatment, with sporadic cases of QTc prolongation. (**b**) Representation of average QTc measured for each experimental group across the duration of treatment, indicating an increase of QTc, but at an insignificant level.

Fig 3. Comparison of QTc and HR across experimental Groups for significance. Correlations of heart rate and QTc (**a**) and correlation of RR interval and QTc (**b**), indicating a general positive correlation between heart rate and QTc. (**c**) Correlation of baseline QTc values obtained before methamphetamine treatment with peak QTc measurements obtained during the course of the treatment, suggesting a general prolongation of QTc. (**d**) Odds analysis of ECG parameters, indicating the likelihood of significant changes before and after methamphetamine treatment. As shown, RTc, QTc, and heart rate indicate significant changes with OR>2.5.

260 ## Sporadic dysregulation of ST interval and other ECG
261 characteristics after Meth treatment

262 While certain ECG parameters do not display significance between treatment groups, an
263 analysis into the variability of these parameters revealed interesting results. Notably, the
264 variability in ST interval increases at higher concentrations (**Fig 4**). While the mean ST interval
265 calculated was not significantly different at all Meth concentrations, the sporadic presence of
266 increasing ST interval duration as Meth concentration increases indicated the propensity of ST
267 interval to vary after Meth dosage. This pattern was not seen in QTc and heart rate, as the
268 variation of both parameters remain similar throughout all treatment groups. Interestingly, RTc
269 also displayed a similar variation to ST, but the difference in RTc may be attributed to ST. While
270 the significance of a prolonged ST interval is not well understood, a previous manuscript
271 documented that ST interval prolongation could be associated with left ventricular hypertrophy
272 (22). This could be explained by realizing that the increase in ventricular volume potentially
273 increases the distance that the Purkinje fibers have to cover for both ventricular depolarization
274 and repolarization, increasing the ST interval.

Fig 4. Analysis of specific ECG parameters between experimental groups. Aggregate measurements were plotted for each experimental group for comparative analysis. Based on significance testing, heart rate exhibited significant increases across all experimental groups, supporting that methamphetamine induces increased heart rate in zebrafish. Other parameters (QTc, RTc, and ST) displayed little to no significance across experimental groups. * indicates $p < 0.05$. *ns* indicates no significance.

275 ## Ion channel dysfunction associated with Meth treatment

276 While we did not observe significant changes in ECG signals between Meth treated and
277 untreated groups aside from heart rate, we wanted to determine if Meth has induced cardiotoxic
278 damage in cardiac tissue. Through our dot blot analysis to detect Meth within zebrafish tissue,
279 we were able to determine that Meth does retain within zebrafish after treatment in a dose-
280 response manner (**Fig 5f**). We chose to investigate and genetic and histological consequences
281 of Meth treatment in zebrafish. To analyze molecular roles of Meth in inducing cardiotoxicity, we
282 conducted RT-PCR of several genes associated with ion channels. These potassium and

283 sodium ion channel genes (*KCNH2*, *KCNQ1*, *SCN5A*) have been selected due to their
284 arrhythmogenic property seen in arrhythmic disorders (23). While the potassium ion channel
285 genes *KCNH2* and *KCNQ1* indicated no significant expression changes, *SCN5A* displayed
286 significant upregulation in the Meth treated groups compared to the untreated group (**Fig. 5a**).
287 *SCN5A* corresponds to the sodium channel protein $Na_v1.5$. Through previous studies involving
288 the characterization of gain-of-function *SCN5A* mutations, upregulation of the sodium ion
289 channel is known to be a factor in several arrhythmic diseases, including Brugada and long QT
290 syndromes, as well as cardiovascular diseases such as cardiac hypertrophy and heart failure
291 (24, 25). Therefore, Meth treatment had been demonstrated to potentially induce arrhythmogenic
292 consequences directly due to dysregulation of certain ion channel expressions and functions.

Fig. 5. Genetic Analysis of Methamphetamine Treatment on Zebrafish. (a) The degree of expression of genetic and epigenetic genes in comparison between experimental groups. Results indicate that MBD1-3, NNMT, EHMT1, DNMT1, and DNMT3A-B exhibit the greatest progressive fold change in expression as methamphetamine dosage treatment increases. SCN5A, a sodium channel gene common in arrhythmic syndromes, has also been upregulated by methamphetamine treatment. (b-d) Quantification of expression changes based on functionality of epigenetic proteins (categorized as DNA methylation, histone methylation and acetylation, and methyl-binding proteins). The protein expression across all categories is increased in methamphetamine treated group (25 μM), with the difference being significant in DNA methylation proteins and methyl-binding proteins. In the panel of genes tested, 29% of genes are associated with DNA methylation, 58% with histone acetylation and methylation, and 13% with methyl-binding proteins. (e) Comparison of protein expression of MBD2, a methyl-binding protein, producing the most pronounced difference in expression between control and 25 μM treated group. (f) Dot blot diagram of methamphetamine detection retained in zebrafish tissue, indicating that methamphetamine does retain in zebrafish tissue in a dose-dependent response. (g) Representative trichrome-stained cardiac sections from zebrafish treated at various concentrations of methamphetamine. Red and pink stains from Biebrich scarlet-acid fuchsin dye indicate cardiac muscle tissue. Blue stains from the aniline blue dye indicate collagen fibers from scar tissue. White arrows and dashed box indicate the locations of collagen deposition in the cardiac tissue. Overall, cardiac tissue derived from zebrafish treated at higher concentrations (40 μM and 50 μM) displayed more tissue injury due to higher collagen deposition than lower concentrations. Scale bar = 500 μm. * indicates significance with $p < 0.05$. ns indicates no significance.

293 **Transcriptional repression as an epigenetic change due to Meth**
294 **treatment**

295 To further analyze the genetic consequences of Meth treatment, we determined the expression
296 changes of epigenetic factors in zebrafish after Meth treatment. From our analysis, the most
297 noteworthy result shown was the expression change in *MBD2*. Zebrafish treated with 25 μM
298 Meth resulted in an approximately 3-fold change in *MBD2* compared to those in the control group
299 (**Fig 5e**). *MBD2* corresponds a transcriptional repressor that specifically binds to CpG sites
300 formed from DNA methylation, so the upregulation of *MBD2* is an implication of long-term
301 repression of genes. Analysis of other potential epigenetic factors potentially affected by Meth
302 treatment yielded similar results. In the diagram depicted in **Fig 5a**, the factors that have
303 underwent a significant fold change (by at least 2 fold) include *MBD1-3*, *NNMT*, *EHMT1*, *DNMT1*,
304 and *DNMT3A-B*. These factors are mainly involved in the various forms of methylation, including
305 DNA methylation and histone methylation. These results were also supported through our
306 quantification of the expression of DNA methylation, histone modifications, and methyl-binding
307 proteins between the control group and the 25 μM treatment group (**Fig 5b-d**). As demonstrated
308 in a previous study analyzing epigenetic influences in *SCN5A* expression, *SCN5A* dysregulation
309 was associated with epigenetic regulations (26). Thus, the upregulation of DNA methylation
310 could potentially be linked with the dysregulation of pertinent ion channel genes such as *SCN5A*.
311 Interestingly, our results yielded a significant difference between the control and treatment
312 groups for DNA methylation and methyl-binding proteins, but not for histone modifications.
313 Histone modifications are generally associated with short-term, reversible forms of genetic
314 repression, whereas DNA methylation is correlated with long-term and stable genetic repression
315 (27). Masson's trichrome stains were performed in cardiac cryosections in which myocardial
316 fibrosis are indicated in blue at 40 and 50 μM of Meth, compared to that of control (0 μM) and

317 25 μM of Meth (**Fig. 5h**). These results were also corroborated through our histological analysis,
318 by specific antibodies in fluorescent immunohistochemistry (**Fig 6**), further supporting that Meth
319 induces an upregulation in both DNA methylation and subsequent transcriptional repression.

Fig. 6. Representative Immunostaining of Methamphetamine and Epigenetic Proteins. (a) Brightfield image of zebrafish heart tissue section. (b-d) Immunostaining of methamphetamine (b), DMNT (c), and MBD (d) within cardiac tissue derived from methamphetamine-treated zebrafish. Antibodies were conjugated with Alexa Fluor 488 to indicate presence of proteins with green fluorescence. The immunostaining figures indicate the retention of methamphetamine after treatment, as well as the upregulation of DMNT, a DNA methylation protein, and MBD, a transcriptional repressor in response to DNA methylation. Scale bar = 100 μm.

320

321 Discussion

322 The Meth epidemic continues to fester worldwide, and cardiovascular diseases are the
323 leading cause of death for Meth abusers. Utilizing animal models to study cardiovascular
324 associated mechanisms could be critical in devising treatments for Meth associated diseases.
325 The zebrafish is an excellent model for drug screening studies due to high fecundity, low
326 maintenance, and similar genetic homology to that in humans. As the zebrafish model is
327 constantly evolving, studies have continued to delineate the applicability of the zebrafish in
328 human medical research. During the initial conception of this study, we have sought to 1.
329 Establish the zebrafish model as an adequate model of drug screening for cardiotoxic effects,
330 and 2. Elucidate the role of Meth in inducing long-term cardiotoxic effects. Utilizing our custom-
331 built zebrafish ECG acquisition system in our lab, we were able to acquire ECG from zebrafish
332 during the two-week treatment period with Meth. Based on our results, we determined that heart
333 rate has increased significantly during the two-week period due to Meth treatment through
334 comparison of heart rate between zebrafish treated with Meth and zebrafish that were treated in

335 normal fish water. Additionally, we conducted an analysis on possible gene targets of Meth that
336 are associated with cardiotoxicity and discovered that *SCN5A*, a cardiac sodium ion channel
337 gene commonly associated with arrhythmogenic syndromes, was significantly upregulated due
338 to Meth treatment. Previous studies have shown that deregulation of these genes have resulted
339 in deterioration in cardiac physiology, including the presence of prolonged QTc (28). These
340 results were consistent with previous human case studies (1). Additionally, we have conducted
341 some experiments to analyze possible Meth-induced epigenetic changes, and results indicated
342 that Meth intake was correlated with an increased amount of DNA methylation and associated
343 gene repression. Similar results have been documented for Meth-induced addiction studies in
344 other animal models (29, 30). While hypermethylation could possibly be associated with the
345 upregulation of ion channel genes and the subsequent dysregulation of cardiac rhythm, the exact
346 mechanism linking these epigenetic and physiological changes remains unknown. In the future,
347 experiments should be conducted to determine the gene targets of hypermethylation.
348 Nevertheless, our results have indicated the propensity of Meth to induce cardiotoxicity in
349 zebrafish through genetic and epigenetic means.

350 While some associations have been determined between Meth treatment and pathologic
351 symptoms shown on ECG in zebrafish, the significance is not very evident. For example, there
352 is currently no explanation on why a dose-response increase in Meth was not seen in certain
353 relevant parameters in ECG. While the dose-response was evident when measuring heart rate,
354 the determination of significance in other parameters was less apparent, such as the presence
355 of QTc changes in response to variations of treated Meth concentrations. QTc prolongation has
356 long been regarded as a prominent symptom in Meth users, and in some isolated cases in this
357 study, QTc prolongation can be seen on ECG signals. However, statistical analysis indicated
358 that there were no significant QTc changes due to Meth treatment. Despite the lack of

359 significance, Meth was confirmed to successfully retain within the zebrafish after treatment, as
360 verified by our dot blot experiment. Meth retention in zebrafish was also demonstrated in a
361 previous zebrafish study (31). We surmise that Meth might pose an antagonizing interaction with
362 tricaine, the anesthetic agent used to acquire ECG. Both Meth and tricaine have opposing
363 mechanisms, as Meth is a stimulant while tricaine is an established anesthetic, known for
364 preventing action potential firing by blocking voltage-gated sodium channels (32). Tricaine has
365 also been shown to prolong the Q-T interval as well, which could also confound zebrafish ECG
366 results (33). Most zebrafish Meth studies focused on the neuropsychological effects of Meth,
367 which were conducted using behavioral tests and without the need for tricaine (34). Therefore,
368 future improvements should be implemented to reduce the effect of tricaine for zebrafish
369 cardiotoxic studies, as tricaine could introduce confounding circumstances, especially when
370 testing psychostimulants on zebrafish. Future studies should also seek to explain the effect of
371 these chemical entities on ion channel function through analysis of sodium and calcium
372 transients for zebrafish. These future experiments would determine the mechanism of Meth in
373 inducing cardiotoxicity as well as bolster the use of zebrafish as a suitable model for cardiotoxic
374 studies.

375 Additionally, future directions would also include linking neurotransmitter response to
376 cardiovascular abnormalities in zebrafish as well as an investigation on ion channel function in
377 the heart after Meth administration. The zebrafish model has already been utilized in numerous
378 Meth studies, mostly related to behavioral studies due to Meth's known ability to disrupt
379 dopamine release and reuptake, thus increasing dopamine expression (35). Therefore, it would
380 be intriguing to understand the role of dopamine in Meth-induced cardiotoxicity, as it would
381 explain whether Meth-induced cardiotoxicity is caused by dopamine or through a direct effect
382 from Meth. One consequence of dopamine response is the change in ion channel expression.

383 Studies have shown the modulation of L-type calcium channels by Meth, but it is not fully
384 understood whether Meth alters calcium channel function directly or via dopamine (30, 36, 37).
385 Overall, more future studies should be planned to elucidate the mechanism of Meth-induced
386 cardiotoxicity.
387

388 # Acknowledgements

389 The authors would like to acknowledge the financial support from the NSF CAREER
390 Award #1917105 (H.C.), the NSF #1936519 (J.L. and H.C), and the NIH SBIR grant
391 #R44OD024874 (M.P.H.L and H.C.).
392

References

1. Kevil CG, Goeders NE, Woolard MD, Bhuiyan MS, Dominic P, Kolluru GK, et al. Methamphetamine Use and Cardiovascular Disease. Arteriosclerosis, Thrombosis, and Vascular Biology. 2019;39(9):1739-46.
2. Won S, Hong RA, Shohet RV, Seto TB, Parikh NI. Methamphetamine-associated cardiomyopathy. Clin Cardiol. 2013;36(12):737-42.
3. Varner KJ, Ogden BA, Delcarpio J, Meleg-Smith S. Cardiovascular Responses Elicited by the “Binge” Administration of Methamphetamine. Journal of Pharmacology and Experimental Therapeutics. 2002;301(1):152-9.
4. Heal DJ, Smith SL, Gosden J, Nutt DJ. Amphetamine, past and present--a pharmacological and clinical perspective. J Psychopharmacol. 2013;27(6):479-96.
5. Kirkpatrick MG, Gunderson EW, Johanson C-E, Levin FR, Foltin RW, Hart CL. Comparison of intranasal methamphetamine and d-amphetamine self-administration by humans. Addiction (Abingdon, England). 2012;107(4):783-91.
6. Robertson SD, Matthies HJ, Galli A. A closer look at amphetamine-induced reverse transport and trafficking of the dopamine and norepinephrine transporters. Molecular neurobiology. 2009;39(2):73-80.
7. Fleckenstein AE, Volz TJ, Riddle EL, Gibb JW, Hanson GR. New insights into the mechanism of action of amphetamines. Annual review of pharmacology and toxicology. 2007;47:681-98.
8. Paratz ED, Cunningham NJ, MacIsaac AI. The Cardiac Complications of Methamphetamines. Heart, Lung and Circulation. 2016;25(4):325-32.
9. Islam MN, Kuroki H, Hongcheng B, Ogura Y, Kawaguchi N, Onishi S, et al. Cardiac lesions and their reversibility after long term administration of methamphetamine. Forensic Science International. 1995;75(1):29-43.
10. Lopez JE, Yeo K, Caputo G, Buonocore M, Schaefer S. Recovery of methamphetamine associated cardiomyopathy predicted by late gadolinium enhanced cardiovascular magnetic resonance. Journal of Cardiovascular Magnetic Resonance. 2009;11(1):46.
11. MacRae CA, Peterson RT. Zebrafish as tools for drug discovery. Nature Reviews Drug Discovery. 2015;14(10):721-31.
12. Cao H, Yu F, Zhao Y, Zhang X, Tai J, Lee J, et al. Wearable multi-channel microelectrode membranes for elucidating electrophysiological phenotypes of injured myocardium. Integrative Biology. 2014;6(8):789-95.
13. Le T, Zhang J, Xia X, Xu X, Clark I, Schmiess-Heine L, et al., editors. Continuous Electrocardiogram Monitoring in Zebrafish with Prolonged Mild Anesthesia. 2020 42nd Annual International Conference of the IEEE Engineering in Medicine & Biology Society (EMBC); 2020 20-24 July 2020.
14. Bazett HC. An Analysis of the Time-Relations of Electrocardiograms. Annals of Noninvasive Electrocardiology. 1997;2(2):177-94.
15. Sander V, Suñe G, Jopling C, Morera C, Belmonte JCI. Isolation and in vitro culture of primary cardiomyocytes from adult zebrafish hearts. Nature Protocols. 2013;8(4):800-9.
16. Khan KM, Collier AD, Meshalkina DA, Kysil EV, Khatsko SL, Kolesnikova T, et al. Zebrafish models in neuropsychopharmacology and CNS drug discovery. British Journal of Pharmacology. 2017;174(13):1925-44.
17. Jiang M, Chen Y, Li C, Peng Q, Fang M, Liu W, et al. Inhibiting effects of rhynchophylline on zebrafish methamphetamine dependence are associated with amelioration

439 of neurotransmitters content and down-regulation of TH and NR2B expression. Progress in
440 Neuro-Psychopharmacology and Biological Psychiatry. 2016;68:31-43.
441 18. Fang M, Peng J, Zhu D, Luo C, Li C, Lin Y, et al. An In Vivo Assessment: Cardiotoxicity
442 Induced by Three Kinds of Addictive Drugs (Methamphetamine, Ketamine, and Methadone) in
443 Zebrafish Embryos. International Journal of Public Health and Safety. 2016;1(3).
444 19. Li J, Li J, Chen Y, Xu Y, Li W, Chen Y, et al. Methamphetamine Use Associated With
445 Monomorphic Ventricular Tachycardia. Journal of Addiction Medicine. 2014;8(6):470-3.
446 20. Kumar S, Sharma R, Kalman JM. Unmasking of familial long QT syndrome type 2 with
447 crystal methamphetamine exposure. Heart Rhythm. 2014;11(10):1836-8.
448 21. Haning W, Goebert D. Electrocardiographic abnormalities in methamphetamine
449 abusers. Addiction. 2007;102(s1):70-5.
450 22. MEAKINS J. PROLONGATION OF THE "S-T" INTERVAL OF THE VENTRICULAR
451 COMPLEX AS SHOWN BY THE ELECTROCARDIOGRAPH. Archives of Internal Medicine.
452 1919;24(5):489-96.
453 23. Brewer KR, Kuenze G, Vanoye CG, George AL, Meiler J, Sanders CR. Structures
454 Illuminate Cardiac Ion Channel Functions in Health and in Long QT Syndrome. Frontiers in
455 Pharmacology. 2020;11(550).
456 24. Li W, Yin L, Shen C, Hu K, Ge J, Sun A. SCN5A Variants: Association With Cardiac
457 Disorders. Front Physiol. 2018;9:1372-.
458 25. Wilde AAM, Amin AS. Clinical Spectrum of SCN5A Mutations: Long QT Syndrome,
459 Brugada Syndrome, and Cardiomyopathy. JACC Clinical electrophysiology. 2018;4(5):569-79.
460 26. Carreras D, Martinez-Moreno R, Pinsach-Abuin Ml, Santafe M, Gomà P, Brugada R, et
461 al. Epigenetic Changes Governing Scn5a Expression in Denervated Skeletal Muscle. Int J Mol
462 Sci. 2021;22:2755.
463 27. Cedar H, Bergman Y. Linking DNA methylation and histone modification: patterns and
464 paradigms. Nature Reviews Genetics. 2009;10(5):295-304.
465 28. Wang T, Wehrens XHT. Enhanced impact of SCN5A mutation associated with long QT
466 syndrome in fetal splice isoform. Heart rhythm. 2012;9(4):598-9.
467 29. Li H, Chen J-A, Ding Q-Z, Lu G-Y, Wu N, Su R-B, et al. Behavioral sensitization induced
468 by methamphetamine causes differential alterations in gene expression and histone
469 acetylation of the prefrontal cortex in rats. BMC Neuroscience. 2021;22(1):24.
470 30. Limanaqi F, Gambardella S, Biagioni F, Busceti CL, Fornai F. Epigenetic Effects
471 Induced by Methamphetamine and Methamphetamine-Dependent Oxidative Stress. Oxidative
472 Medicine and Cellular Longevity. 2018;2018:4982453.
473 31. Yin X, Guo C, Lv J, Hou S, Zhang Y, Jin X, et al. Biomimetic Accumulation of
474 Methamphetamine and Its Metabolite Amphetamine by Diffusive Gradients in Thin Films to
475 Estimate Their Bioavailability in Zebrafish. Environmental Science & Technology Letters.
476 2019;6(12):708-13.
477 32. Scholz A. Mechanisms of (local) anaesthetics on voltage-gated sodium and other ion
478 channels. British Journal of Anaesthesia. 2002;89(1):52-61.
479 33. Cakir Y, Strauch SM. Tricaine (MS-222) is a safe anesthetic compound compared to
480 benzocaine and pentobarbital to induce anesthesia in leopard frogs (Rana pipiens).
481 Pharmacological reports : PR. 2005;57(4):467-74.
482 34. Mi G, Gao Y, Yan H, Jin X, Ye E, Liu S, et al. l-Scoulerine attenuates behavioural
483 changes induced by methamphetamine in zebrafish and mice. Behavioural Brain Research.
484 2016;298:97-104.
485 35. Hedges DM, Obray JD, Yorgason JT, Jang EY, Weerasekara VK, Uys JD, et al.
486 Methamphetamine Induces Dopamine Release in the Nucleus Accumbens Through a Sigma
487 Receptor-Mediated Pathway. Neuropsychopharmacology. 2018;43(6):1405-14.

488 36. Sugimoto K, Okamura K, Tanaka H, Takashima S, Ochi H, Yamamoto T, et al.
489 Methamphetamine directly accelerates beating rate in cardiomyocytes by increasing Ca2+
490 entry via L-type Ca2+ channel. Biochemical and Biophysical Research Communications.
491 2009;390(4):1214-20.
492 37. Hernandez-Lopez S, Tkatch T, Perez-Garci E, Galarraga E, Bargas J, Hamm H, et al.
493 D2 dopamine receptors in striatal medium spiny neurons reduce L-type Ca2+ currents and
494 excitability via a novel PLC[beta]1-IP3-calcineurin-signaling cascade. The Journal of
495 neuroscience : the official journal of the Society for Neuroscience. 2000;20(24):8987-95.
496

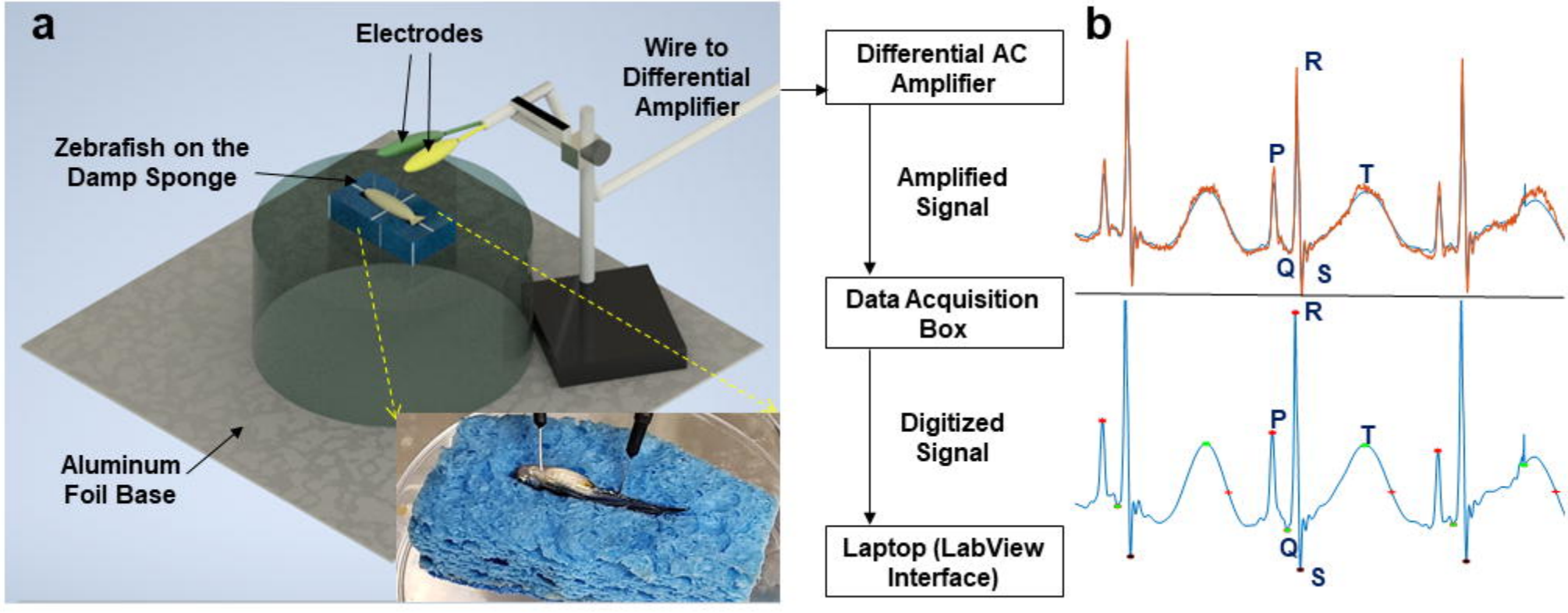
a
Electrodes
Wire to Differential Amplifier
Zebrafish on the Damp Sponge
Aluminum Foil Base
Differential AC Amplifier
Amplified Signal
Data Acquisition Box
Digitized Signal
Laptop (LabView Interface)
b
R
P
T
Q
S
R
P
T
Q
S

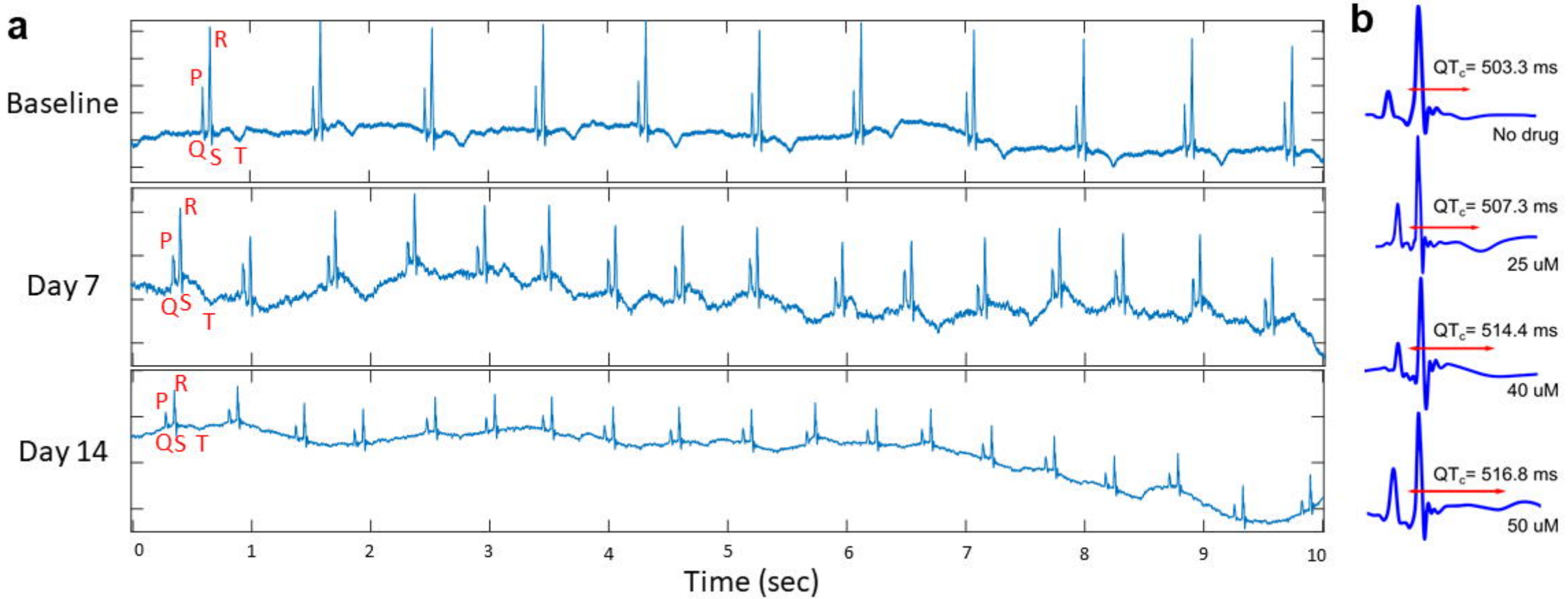
a
Baseline
Day 7
Day 14
P
R
Q
S
T
0
1
2
3
4
5
6
7
8
9
10
Time (sec)
b
QTc= 503.3 ms
No drug
QTc= 507.3 ms
25 uM
QTc= 514.4 ms
40 uM
QTc= 516.8 ms
50 uM

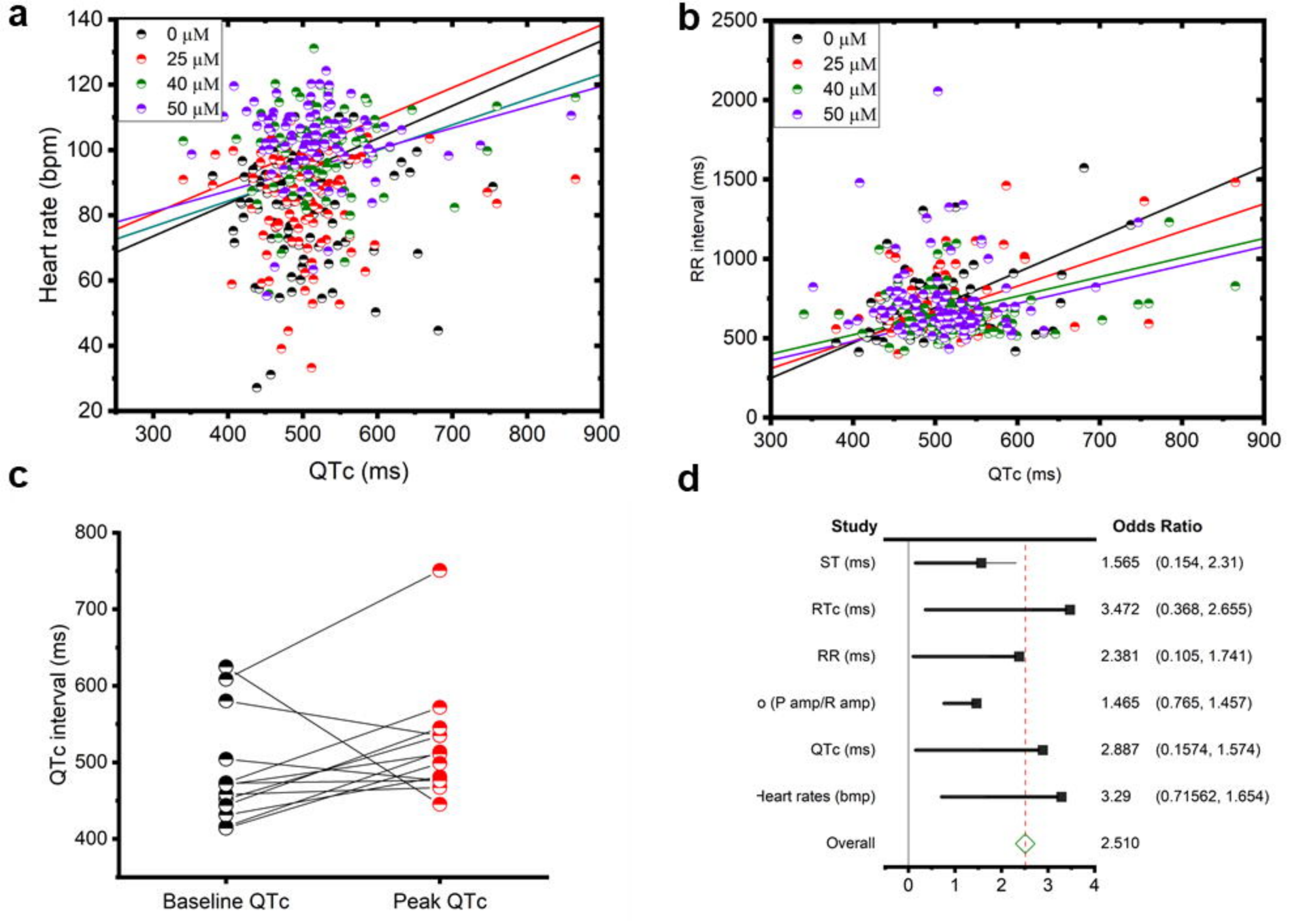
a
0 μM
25 μM
40 μM
50 μM
Heart rate (bpm)
QTc (ms)
b
0 μM
25 μM
40 μM
50 μM
RR interval (ms)
QTc (ms)
c
QTc interval (ms)
Baseline QTc
Peak QTc
d
Study
Odds Ratio
ST (ms) 1.565 (0.154, 2.31)
RTc (ms) 3.472 (0.368, 2.655)
RR (ms) 2.381 (0.105, 1.741)
o (P amp/R amp) 1.465 (0.765, 1.457)
QTc (ms) 2.887 (0.1574, 1.574)
-leart rates (bmp) 3.29 (0.71562, 1.654)
Overall 2.510

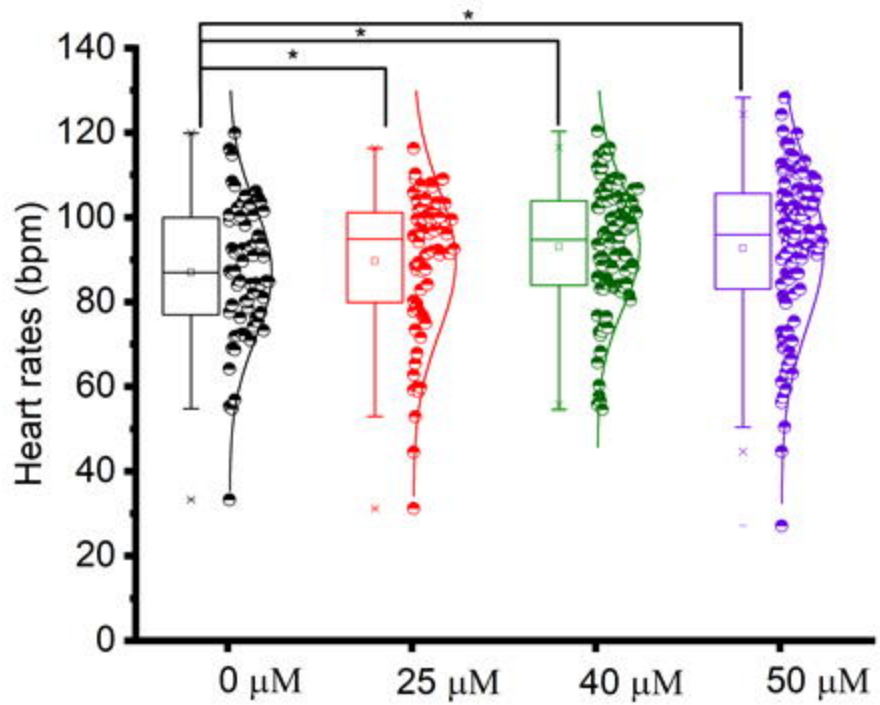
Heart rates (bpm)
0
20
40
60
80
100
120
140
*
*
*
0 μM
25 μM
40 μM
50 μM

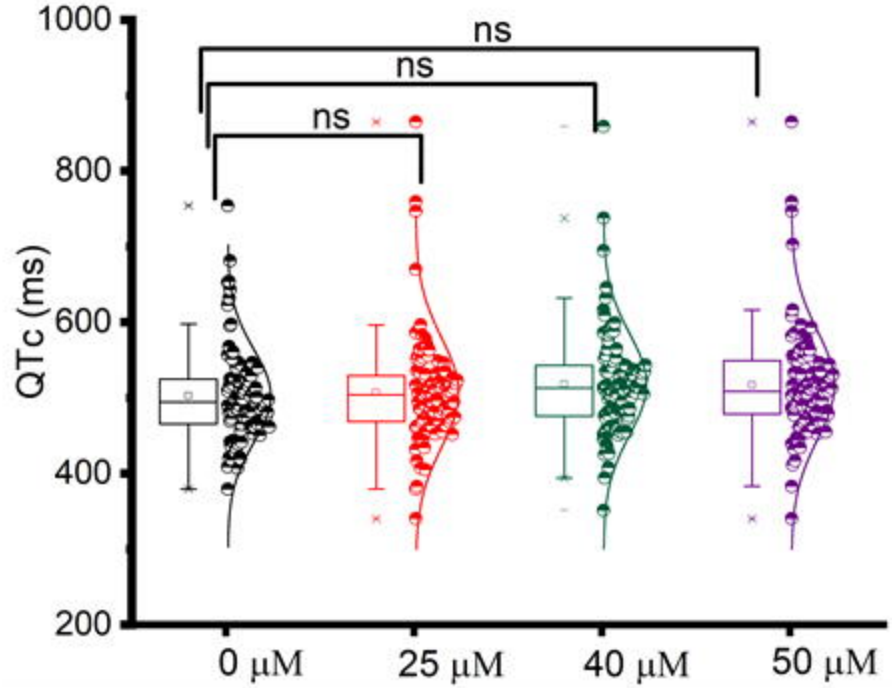
QTc (ms)
200
400
600
800
1000
ns
ns
ns
0 μM
25 μM
40 μM
50 μM

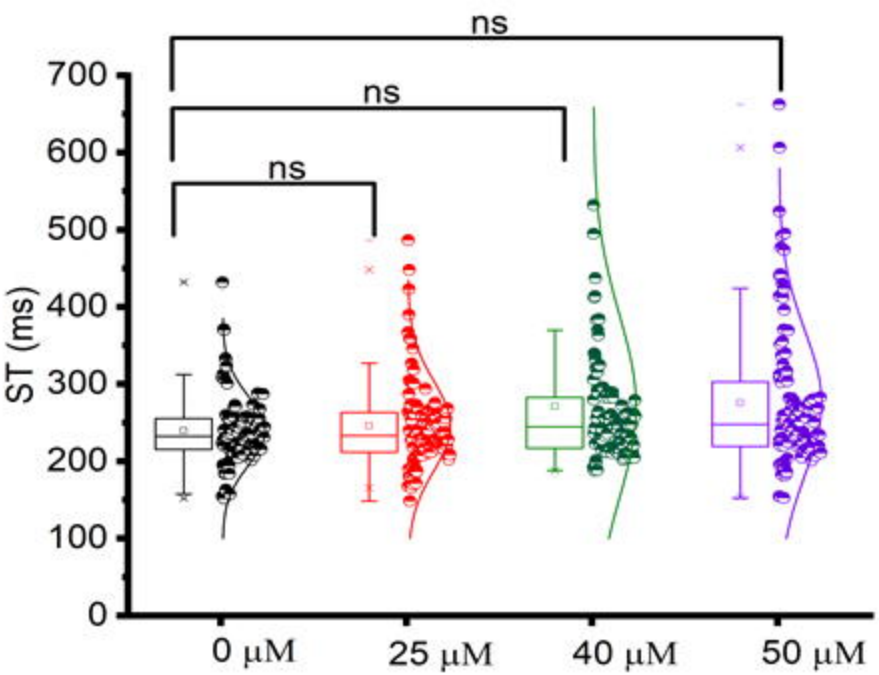
ST (ms)
0
100
200
300
400
500
600
700
ns
ns
ns
0 μM
25 μM
40 μM
50 μM

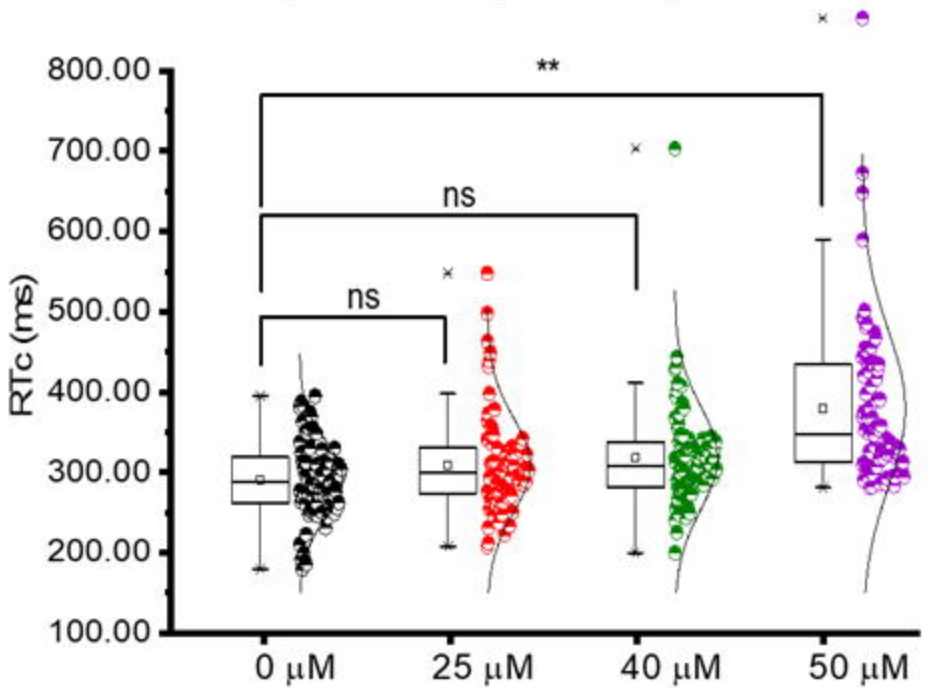
RTc (ms)
100.00
200.00
300.00
400.00
500.00
600.00
700.00
800.00
**
ns
ns
0 μM
25 μM
40 μM
50 μM

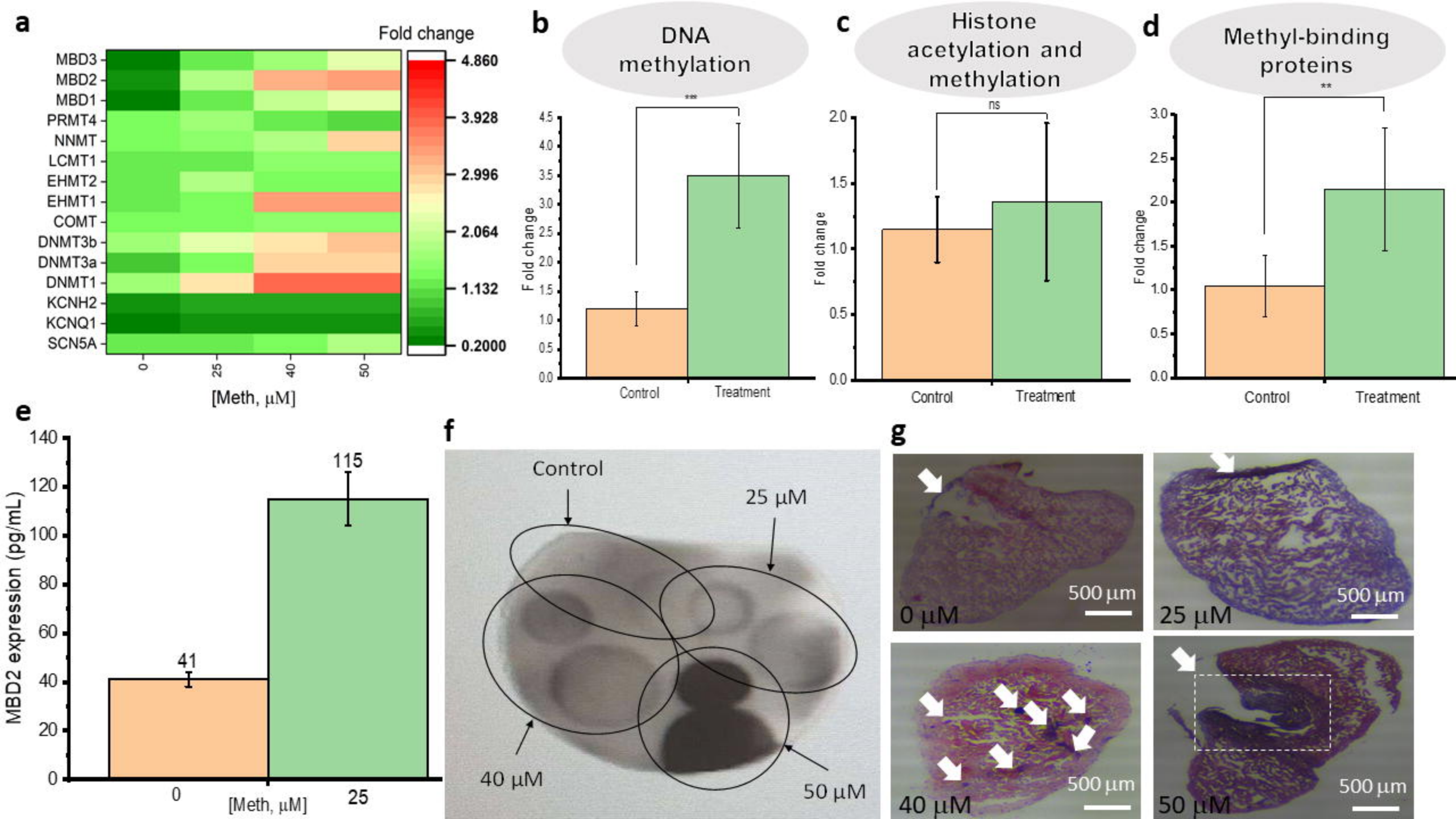
a
Fold change
MBD3
MBD2
MBD1
PRMT4
NNMT
LCMT1
EHMT2
EHMT1
COMT
DNMT3b
DNMT3a
DNMT1
KCNH2
KCNQ1
SCN5A
4.860
3.928
2.996
2.064
1.132
0.2000
0
25
40
50
[Meth, μM]
b
DNA methylation
**
Fold change
Control
Treatment
c
Histone acetylation and methylation
ns
Fold change
Control
Treatment
d
Methyl-binding proteins
**
Fold change
Control
Treatment
e
MBD2 expression (pg/mL)
41
115
0
25
[Meth, μM]
f
Control
25 μM
40 μM
50 μM
g
0 μM
25 μM
40 μM
50 μM
500 μm

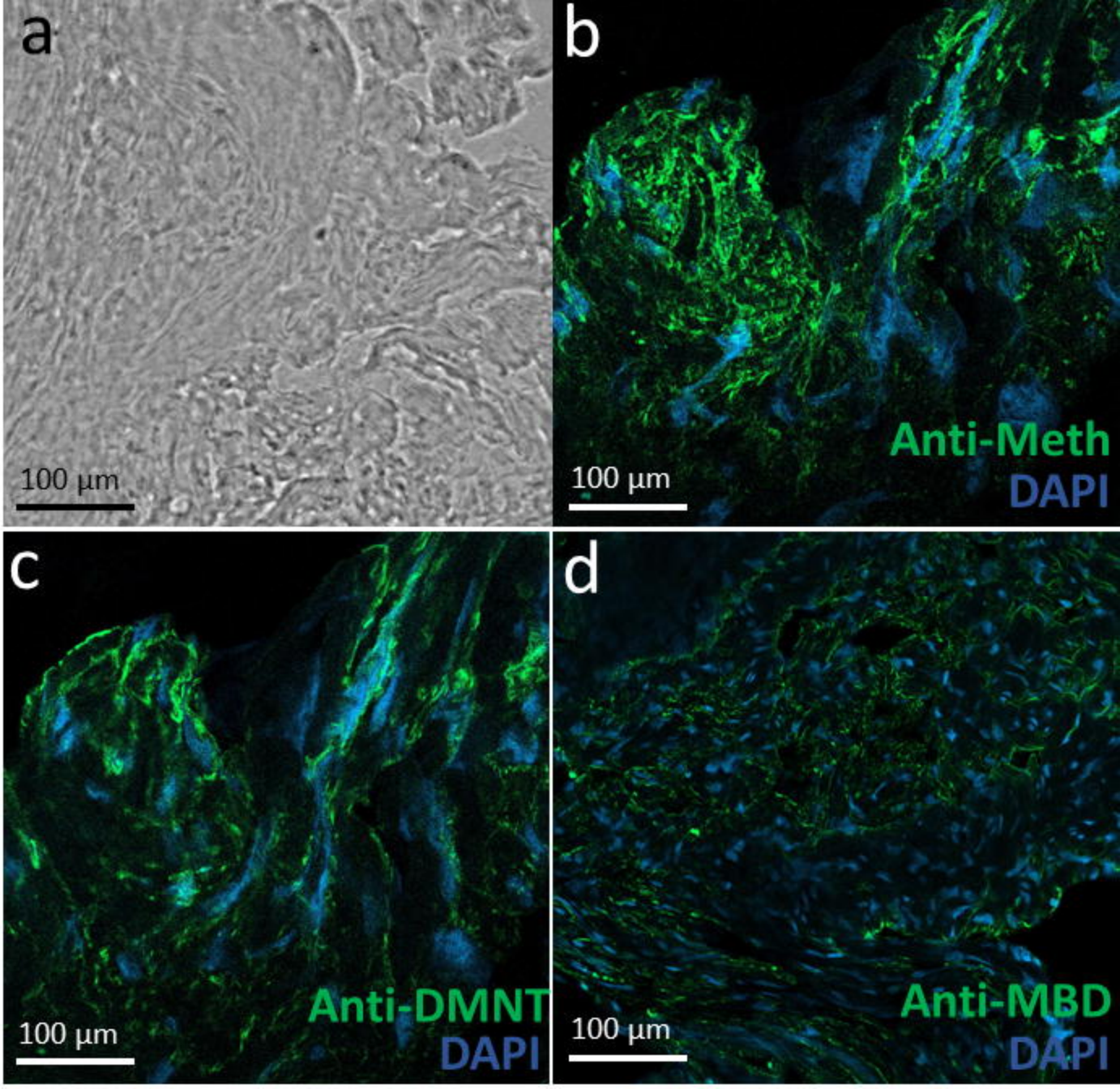
a
100 µm
b
Anti-Meth
DAPI
100 µm
c
Anti-DMNT
DAPI
100 µm
d
Anti-MBD
DAPI
100 µm